Citation: CPT Pharmacometrics Syst. Pharmacol. (2016) 5, 665–673; doi:10.1002/psp4.12137

ORIGINAL ARTICLE

Integrated Two-Analyte Population Pharmacokinetic Model for Antibody–Drug Conjugates in Patients: Implications for Reducing Pharmacokinetic Sampling

D Lu[1]*, L Gibiansky[2], P Agarwal[1], RC Dere[1], C Li[1], Y-W Chu[1], J Hirata[1], A Joshi[1], JY Jin[1] and S Girish[1]

An integrated pharmacokinetics (PK) model that simultaneously describes concentrations of total antibody (Tab) and antibody-conjugated monomethyl auristatin E (acMMAE) following administration of monomethyl auristatin E (MMAE)-containing antibody–drug conjugates (ADCs) was developed based on phase I PK data with extensive sampling for two ADCs. Two linear two-compartment models that shared all parameters were used to describe the PK of Tab and acMMAE, except that the deconjugation rate was an additional clearance pathway included in the acMMAE PK model compared to Tab. Further, the model demonstrated its ability to predict Tab concentrations and PK parameters based on observed acMMAE PK and various reduced or eliminated Tab PK sampling schemes of phase II data. Thus, this integrated model allows for the reduction of Tab PK sampling in late-phase clinical development without compromising Tab PK characterization.
CPT Pharmacometrics Syst. Pharmacol. (2016) **5**, 665–673; doi:10.1002/psp4.12137; published online 10 November 2016.

Study Highlights

WHAT IS THE CURRENT KNOWLEDGE ON THE TOPIC?

☑ Multiple analytes are quantified following dosing of MMAE containing ADCs. However, an integrated multiple-analyte PK model based on the clinical data has not yet been developed or used for PK sampling reductions in clinical studies.

WHAT QUESTION DOES THIS STUDY ADDRESS?

☑ Whether an integrated model can simultaneously describe PK of Tab and conjugate (acMMAE) and enable PK sampling reduction/elimination for one analyte, based on its quantitative relationship with another analyte.

WHAT THIS STUDY ADDS TO OUR KNOWLEDGE

☑ A simplified integrated population PK model can simultaneously describe the PK of Tab and conjugate (acMMAE), which can adequately predict the PK of Tab based on reduced/eliminated PK sampling of Tab and original intensive sampling of acMMAE PK data.

HOW MIGHT THIS CHANGE DRUG DISCOVERY, DEVELOPMENT, AND/OR THERAPEUTICS?

☑ The model is useful to quantify the relationship of multiple analytes and reduce PK sampling of one analyte in cancer patients for ADCs during late-stage development without compromising the PK characterization, which is more cost-effective for drug development.

Antibody–drug conjugates (ADCs) are novel biologic therapeutics that aim to provide targeted delivery of cytotoxic drugs to tumor cells by linking the drug to a targeting monoclonal antibody (mAb). ADCs combine the targeting properties and favorable pharmacokinetics (PK) of a mAb to improve the therapeutic window of highly potent chemotherapeutic agents. Currently, two ADCs, brentuximab vedotin (Adcetris) and ado-trastuzumab emtansine (Kadcyla), have received regulatory approval in multiple countries. More than 40 ADCs directed against a variety of solid and hematologic tumor targets are currently in different stages of clinical development.[1–5]

When manufacturing ADCs, the conjugation reaction results in a heterogeneous mixture of ADC molecules with different numbers of cytotoxic drugs conjugated to the antibody, referred to as the species with different drug-to-antibody ratios (DARs).[6] ADCs that use a protease-labile di-peptide linker (maleimidocaproyl-valine-citrulline-p-aminobenzoyloxycarbonyl [MC-VC-PABC]) conjugated to monomethyl auristatin E (MMAE) are in clinical development.[2,4] MMAE-containing ADCs generally consist of species with even-numbered DARs (0, 2, 4, 6, or 8), with DAR species 2 and 4 being the most abundant.[6]

Given the complicated structure of ADCs, which contain both large and small molecule components, and a mixture of various DAR species in the dosing solution, the PK of ADCs are expected to be complex. ADCs are considered to be catabolized through two major pathways: proteolytic degradation and deconjugation.[7] The proteolytic degradation pathway leads to the catabolism of ADC to amino acids and the unconjugated drug, and is likely mediated by target-specific or nonspecific cellular uptake followed by subsequent lysosomal degradation. The deconjugation clearance leads to the formation of unconjugated antibody and the drug, and is likely mediated by chemical and enzymatic processes (e.g., maleimide exchange).[7,8] It is expected that ADC catabolism and deconjugation *in vivo* changes the concentration and relative fractions of

[1]Genentech Inc., South San Francisco, California, USA; [2]QuantPharm LLC, North Potomac, Maryland, USA. *Correspondence: D Lu (lu.dan@gene.com)
Received 20 April 2016; accepted 10 September 2016; published online on 10 November 2016. doi:10.1002/psp4.12137

individual DAR species with time, by converting high DAR species to low DAR species, resulting in a gradual decrease in average DAR over time. This phenomenon was observed in a preclinical study.[9]

Considering the heterogeneity and complex changes in ADC concentration and composition after ADC administration, multiple analytes have been measured in order to characterize the PK properties of an ADC.[6,10] These measurements include: Tab (sum of conjugated, partially deconjugated, and fully deconjugated antibody); naked antibody (antibody without the conjugated drug); conjugate (evaluated as either conjugated-antibody or antibody-conjugated drug); and the unconjugated drug.[6,10–12] For MMAE containing ADCs currently in clinical development at Genentech, three analytes are routinely measured for PK assessment: total antibody (Tab), conjugate (evaluated as antibody-conjugated MMAE, acMMAE), and unconjugated MMAE. It has been observed that the PK of Tab and acMMAE were largely similar, suggesting that the conjugate PK is mainly driven by its antibody component (https://ash.confex.com/ash/2013/webprogram/Paper62229.html).[13] The exposures of both analytes are correlated with objective response rate and incidence of grade $\geq$2 peripheral neuropathy (unpublished data, Genentech, and https://ash.confex.com/ash/2015/webprogram/Paper78428.html). In contrast, unconjugated MMAE exposure is very low (https://ash.confex.com/ash/2013/webprogram/Paper62229.html)[13] and no strong correlations with objective response rate and incidence of grade $\geq$2 peripheral neuropathy have been shown to date (unpublished data, Genentech). Given the high potency of MMAE, further assessments are needed. All three analytes are of significant clinical importance when trying to understand the driver of clinical efficacy and safety.

Hypothetically, while deconjugation contributes to the elimination of acMMAE but not Tab, both Tab and acMMAE are considered to be eliminated by proteolytic degradation. Thus, an estimation of deconjugation clearance using an integrated Tab-acMMAE PK model could potentially allow for the prediction of Tab PK based on acMMAE PK, to reduce or eliminate Tab PK sampling in late-phase clinical development.

Semimechanistic integrated Tab-conjugate PK models that are based on the major ADC catabolism pathways described above to simultaneously fit multiple PK analytes have been developed for some ADCs based on preclinical (https://ash.confex.com/ash/2013/webprogram/Paper62229.html)[7,9,14] and clinical data.[15,16] These models shed light on the ADC catabolism, as well as the unconjugated cytotoxic drug formation pathways after administration of an ADC *in vivo*. However, the application of these models to optimize PK sampling and thereby reduce the number of analytes in a clinical setting are limited to a single publication in the literature, which fits Tab and cytotoxic drug conjugated antibody simultaneously after dosing of Kadcyla to patients.[16] However, there is currently no literature on a model that fits Tab and antibody-conjugated cytotoxic drugs (e.g., acMMAE) simultaneously using clinical data, although there is some work using preclinical data.[7,17]

The analyses described here have three major goals. First, to demonstrate that the theoretical integrated Tab-acMMAE PK model[18] is applicable to real clinical data. Second, to investigate whether the final integrated model may allow for the prediction of Tab PK based on the observed acMMAE PK data. If successful, this approach would allow for characterization of Tab and acMMAE PK with reduced or even completely eliminated sampling of Tab in late-phase trials without compromising its PK characterization. Given that two separate blood samples were needed for the quantification of serum Tab concentrations and plasma acMMAE and unconjugated MMAE concentrations, eliminating Tab PK sampling would greatly reduce the burden for patients. Third, to demonstrate that the proposed methods are likely applicable to the entire MMAE ADC platform, by using simultaneous modeling of clinical data from two MMAE ADCs. Given these major goals, a relatively simple population PK model without covariates is more desirable, thus the covariate assessment was not performed.

Two MMAE-containing ADCs pinatuzumab vedotin and polatuzumab vedotin (https://ash.confex.com/ash/2013/webprogram/Paper62229.html, https://ash.confex.com/ash/2014/webprogram/Paper72975.html)[13,19] that target the different lineages of B-cell antigens, namely, cluster of differentiation (CD)−22 and CD79b, respectively, were used for this analysis. Both are currently in clinical development for treating B-cell lymphoma. Both are also mixtures of antibodies linked with 0, 2, 4, 6, or 8 MMAE molecules via the MC-VC-PABC linker, with a mean drug-to-antibody ratio (mDAR) of 3.585, measured by hydrophobic interaction chromatography (HIC) (unpublished data, Genentech). These two ADCs have the same linker and cytotoxic component, and have an overall similar PK for Tab, acMMAE, and unconjugated MMAE (https://ash.confex.com/ash/2013/webprogram/Paper62229.html).[13]

METHODS

Study designs and data

Data from non-Hodgkin's lymphoma patients from three clinical studies (**Supplemental Table 1**) were used to develop the model. The studies were approved by the Medical Ethics Committee and were carried out according to the International Conference on Harmonization guidelines for good clinical practice (http://www.ich.org/home.html). PK concentrations of Tab, acMMAE, and unconjugated MMAE were quantified in clinical studies at prespecified timepoints. The current two-analyte integrated PK model used data for Tab and acMMAE.

More than 35 serum and plasma samples (more than 70 samples in total) per patient were obtained from the phase I single-agent studies for pinatuzumab vedotin (DCT4862g) and polatuzumab vedotin (DCS4968g) for ADC PK assessment, and more than 30 serum and plasma samples (more than 60 samples in total) per patient were obtained from the combination with rituximab cohorts (**Supplemental Table 1**). These samples included intensive PK samples in the first four cycles, in addition to predose and peak concentration data throughout the treatment. Inclusion of this extensive PK sampling scheme aimed to fully characterize the distribution, metabolism/catabolism, and elimination of the ADC along with assessing any time-dependent change

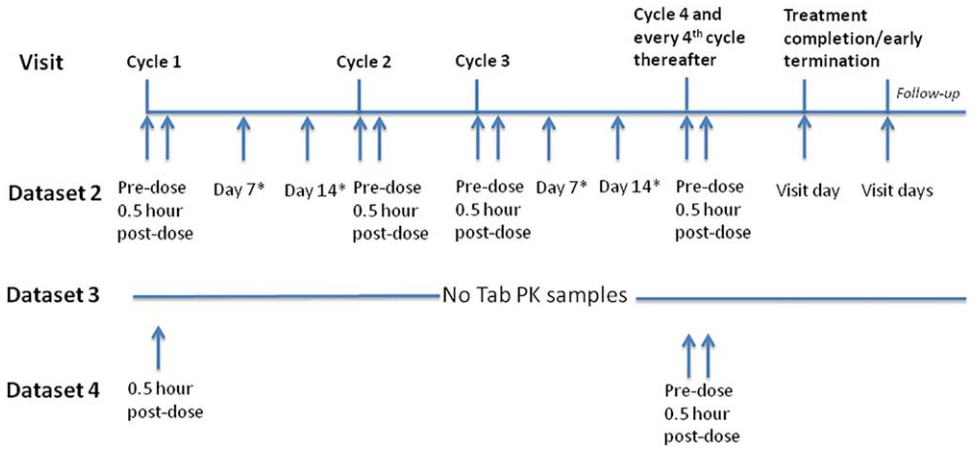

Figure 1 Tab PK sampling scheme for pinatuzumab vedotin and polatuzumab vedotin in the phase II study for original sampling scheme (**dataset 2**), all Tab PK data removed (**dataset 3**) and reduced Tab PK data (**dataset 4**). * Days are referred to as postdose of pinatuzumab vedotin or polatuzumab vedotin. Note: datasets 2, 3, and 4 are phase I data combined with all acMMAE PK data and different sampling schemes of Tab in the phase II study as shown in this figure.

of PK due to target elimination after treatment. A similar PK sampling scheme to that used for the phase I single-agent cohorts was obtained for phase Ib dose escalation cohorts for the ADC in combination with rituximab (**Supplemental Table 1**). For the phase II study GO27834, more than 15 serum and plasma samples (total of more than 30 samples) per patient were obtained for ADC PK assessment, in which the ADC was given in combination with rituximab (**Figure 1** and **Supplemental Table 1**). These samples included relatively intensive PK samples in Cycles 1 and 3, and predose and peak concentration data in the first four cycles and every 4th cycle following, to characterize PK of the ADC in the presence of rituximab. It was found that rituximab combination does not impact the PK of ADCs (unpublished data, Genentech).

The phase I data were first used for model development (**dataset 1**, **Supplemental Table 1**) and the phase II data were used to investigate the PK sampling reduction or elimination schemes of Tab, as explained in later sections.

Bioanalytical methods for PK concentrations of multiple analytes

Tab, the concentration of antibody with DAR equals 0 to 8, including fully conjugated, partially deconjugated, and fully deconjugated antibody, were measured in patient serum samples using a validated enzyme-linked immunosorbent assay (ELISA) method. For both ADCs, the anti-complementarity determining region (CDR) specific antibody against anti-CD22 or anti-CD79b antibody was used as the capture reagent. The minimum quantifiable concentration for Tab was 0.06 and 0.05 μg/mL in human serum for pinatuzumab vedotin and polatuzumab vedotin, respectively. The acMMAE concentration represents the total concentration of MMAE conjugated to the antibody moiety. It was measured in patient plasma samples using a validated method consisting of Protein A affinity capture of the conjugate from plasma followed by enzyme-mediated release of MMAE, and liquid chromatography-tandem mass spectrometry (LC-MS/MS) method for detection. The lower limit of quantitation for the acMMAE assay was 0.18 ng/mL and 0.359 ng/mL (MMAE equivalent concentration) in human plasma for pinatuzumab vedotin and polatuzumab vedotin, respectively.

Development and validation of two-analyte integrated population PK model using the phase I data

Several structural models were explored (simplified or non-simplified) and a final simplified model proposed[18] with some modifications was selected for analyzing the clinical data. The published model[18] was established based on simulated data and was derived from the initial 18-compartment model with nine pairs of compartments describing each of the nine DAR species (DAR from 0 to 8); by assuming that 1) proteolytic clearances, intercompartmental clearances, central volumes, and peripheral volumes of all ADC species are independent of the DAR; and 2) the deconjugation rate of each DAR species is linearly proportional to the DAR, i.e., the deconjugation rate of each MMAE molecule from the conjugate (k_{dec}) is independent of the DAR of the conjugate.

The published model[18] contains both linear and nonlinear components for systemic clearance. To describe the phase I PK data of pinatuzumab vedotin and polatuzumab vedotin, only the linear proteolytic clearance was included in the final model, as separate modeling of each analyte indicated that the contribution of nonlinear target-mediated elimination for these two ADCs is negligible at clinically relevant doses in relapsed/refractory lymphoma patients, potentially due to B-cell depletion (unpublished data, Genentech). Some other modifications are introduced as detailed below. The final model structure is shown in **Figure 2**. In this model, the PK of Tab and acMMAE are described by the following differential equations (Eqs. 1–4):

$$dA_1/dt = -(k_{10} + k_{12})A_1 + k_{21}A_2 \quad (1)$$

$$dA_2/dt = k_{12}A_1 - k_{21}A_2 \quad (2)$$

$$dA_3/dt = -(k_{10} + k_{12})A_3 - k_{dec}A_3 + k_{21}A_4 \quad (3)$$

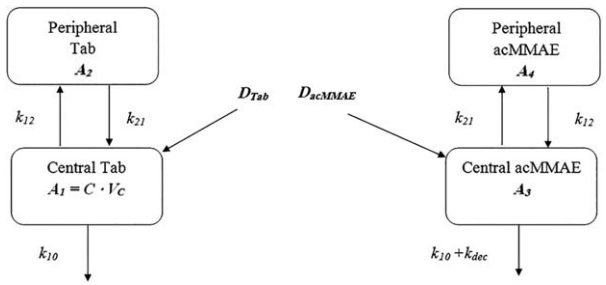

Figure 2 Final integrated Tab - acMMAE PK model structure. A_1 and A_2 are the molar amounts of Tab in the central and peripheral compartments, A_3 and A_4 are the molar amounts of acMMAE in the central and peripheral compartments; $k_{10} = CL/V_C$; $k_{12} = Q/V_C$; $k_{21} = Q/V_P$; CL is proteolytic clearance of the conjugate; Q is intercompartment clearance; V_C is central volume and V_P is peripheral volume; k_{dec} is the deconjugation rate for acMMAE. The initial conditions are: $A_1(0) = D_{Tab}$, $A_2(0) = 0$, $A_3(0) = D_{acMMAE}$, $A_4(0) = 0$. D_{Tab} is the dose of Tab in molar unit; D_{acMMAE} is the dose of acMMAE in molar unit, $D_{acMMAE} = mDAR * D_{Tab}$; mDAR = average drug to antibody ratio of the dosing solution (3.585 for both polatuzumab vedotin and pinatuzumab vedotin).

$$dA_4/dt = k_{12}A_3 - k_{21}A_4 \quad (4)$$

where $k_{10} = CL/V_C$; $k_{12} = Q/V_C$; $k_{21} = Q/V_P$; A_1 and A_2 are the molar amounts of Tab in the central and peripheral compartments, respectively; A_3 and A_4 are the molar amounts of acMMAE in the central and peripheral compartments, respectively; CL is the proteolytic clearance of the conjugate; Q is the intercompartment clearance; V_C is the central volume; V_P is the peripheral volume of distribution; and k_{dec} is the deconjugation rate of a single MMAE molecule from the conjugate. Eqs. 1–4 are supplemented by the following initial conditions and/or dosing information:

$$A_1(0) = D_{Tab},\ A_2(0) = 0,\ A_3(0) = D_{acMMAE},\ A_4(0) = 0$$

where D_{Tab} and D_{acMMAE} are molar amounts of Tab and acMMAE in the dose given to each patient. $D_{acMMAE} = mDAR * D_{Tab}$, and mDAR = 3.585 for both polatuzumab vedotin and pinatuzumab vedotin, which is measured by HIC. It is important to emphasize that Eqs. 1 and 2 that describe Tab and Eqs. 3 and 4 that describe acMMAE share all parameters except for k_{dec}, which is absent in Eq. 1 but present in Eq. 3. The analysis involved two analytes (Tab and acMMAE) with different molecular weights. To allow simultaneous modeling, the dose was converted to molar units (nmol) while nonlinear mixed effect modeling (NONMEM) control stream contained the explicit conversion factor that transformed the model predictions in molar units (nmol/L) to the observed concentrations in mass units (ng/mL).

The PK data of both polatuzumab vedotin and pinatuzumab vedotin were combined in one dataset for the analysis. As ADCs developed using the same platform have similar PK properties (Xu et al., http://www.acop7.org/previous-acop-meetings-acop6), the same structural model was used to describe the integrated PK of both ADCs. A molecule indicator was introduced to allow the estimation of different population values of CL, V_C, and k_{dec} for each molecule, while parameters of the second compartment (Q and V_P), interindividual variability, and residual variability were assumed to be the same for both molecules. The time-dependent clearance was assessed as well.

It was found that the model systemically underestimated the acMMAE concentrations and overestimated Tab concentrations across all timepoints. Exploratory analysis further indicated that the molar ratio based on PK data between Tab and acMMAE at the earlier timepoints postdose (e.g., 0.5 hours post the end of infusion) is higher than the mDAR in the dosing solution measured by HIC, which explained that the systemic fitting bias observed is most likely due to the different assays for mDAR and PK measurements. To account for this bias, a correction factor parameter (CORR) was introduced as follows for fitting the acMMAE concentrations:

$$C_{predicted} = CORR * C_{model} \quad (5)$$

where $C_{predicted}$ is the model prediction by fitting the observed data of acMMAE concentrations, $C_{model} = A_1/V_C$, which is the model prediction of acMMAE concentrations provided by Eqs. 1–4. The CORR can be added to either the model output of Tab or acMMAE, or the dose input of Tab or acMMAE, which are mathematically equivalent for the computation. The CORR was estimated to be different for two ADCs.

The NONMEM control stream is provided in the **Supplemental Material** (**S1**). This model developed based on phase I data (**dataset 1**) will be referred to as **model 1**. Standard goodness-of-fit plots and individual fitting plots were evaluated to assess the model performance.

Assessment of model prediction of Tab PK concentrations and exposure parameters based on reduced or eliminated Tab PK samples

PK data from the phase II study were further used to test the ability of the final model to predict Tab PK concentrations and parameters based on reduced or eliminated Tab PK samples. As shown in **Figure 1**, three additional datasets were constructed by combining the phase I and II data of the two analytes, in the following way: the **dataset 2** contains all phase I and II PK data of Tab and acMMAE; **dataset 3** contains all phase I data, all phase II PK data of acMMAE but no phase II PK data of Tab; **dataset 4** contains all phase I data, all phase II PK data of acMMAE, and reduced sampling of phase II PK data of Tab (3 serum PK samples: 30 minutes post end of infusion of Cycle 1, predose, and 30 minutes post end of infusion of Cycle 4) (**Figure 1** and **Supplemental Table 1**). The structure model (**model 1**) established using the phase I data (**dataset 1**) was refitted to **dataset 2** (**model 2**), **dataset 3** (**model 3**), and **dataset 4** (**model 4**). **model 2** results therefore represent the best-case/benchmarking scenario for the Tab PK parameter estimation when the most abundant Tab data are available. The **model 3** results represent the Tab PK parameter estimation based on the least sampling scenario that no Tab PK data of the phase II study were available. The **model 4** results represent the Tab PK parameter estimation based on the reduced PK sampling scenario of Tab (i.e., ~80% reduction of Tab PK samples compared to the original sampling scheme of more than 15 Tab samples per patient).

Standard goodness-of-fit plots, individual fitting plots, and visual predictive check (VPC)[20] plots (based on 1000 trial

Table 1 Parameter estimates of the final integrated Tab-acMMAE PK Model 1 (fit phase I data only), Model 2 (fit phase I and II data), Model 3 (fit phase I full dataset and phase II data with all Tab PK samples removed), and Model 4 (fit phase I full dataset and phase II data with only limited Tab PK samples retained)

	Model 1		Model 2		Model 3		Model 4	
Description	**Value**	**RSE (%)**	**Value**	**RSE (%)**	**Value**	**RSE (%)**	**Value**	**RSE (%)**
Pinatuzumab vedotin clearance: CL_{pina} (L/hr)	0.0292	15.0	0.0234	10.5	0.0230	11.6	0.0231	11.1
Intercompartment clearance: Q (L/hr)	0.0267	5.97	0.0222	3.79	0.0233	3.39	0.0225	3.56
Pinatuzumab vedotin central volume: $V_{C,pina}$ (L)	5.35	4.03	4.86	3.22	5.06	3.07	4.93	3.20
Peripheral volume: V_P (L)	8.21	7.74	7.8	5.58	8.28	5.29	8.13	5.48
Pinatuzumab vedotin deconjugation rate: $k_{dec,pina}$ (1/hr)	0.00855	4.37	0.00799	2.81	0.0082	3.88	0.00807	3.08
Pinatuzumab vedotin assay correction: $CORR_{pina}$	1.31	1.23	1.27	1.02	1.32	1.16	1.29	1.14
Polatuzumab vedotin clearance: CL_{pola} (L/hr)	0.0355	12.4	0.0253	9.01	0.0276	6.19	0.0261	8.90
Polatuzumab vedotin central volume: $V_{C,pola}$ (L)	5.00	3.73	4.5	2.9	5.02	2.69	4.65	2.92
Polatuzumab vedotin deconjugation rate: $k_{dec,pola}$ (1/hr)	0.00647	3.77	0.0064	2.2	0.00641	3.22	0.00649	2.44
Polatuzumab vedotin assay correction: $CORR_{pola}$	1.45	0.975	1.35	0.767	1.47	0.944	1.39	0.895
Random effect on CL: ω^2_{CL}	0.488	13.2	0.439	7.57	0.477	8.4	0.471	8.02
Random effect on Q: ω^2_{Q}	0.269	13.9	0.193	10.4	0.17	9.85	0.177	10.1
Random effect on V_C: ω^2_{VC}	0.0519	11.5	0.0539	9.2	0.0507	9.41	0.054	9.37
Random effect on V_P: ω^2_{VP}	0.707	14.5	0.458	9.02	0.439	9.53	0.434	9.34
Random effect on k_{dec}: ω^2_{kdec}	0.053	15.7	0.0395	10.0	0.0481	13.4	0.0403	11.0
Residual error for Tab: σ^2_{Tab}	0.0585	1.63	0.0535	1.37	0.0594	1.63	0.0582	1.58
Residual error for acMMAE: σ^2_{acMMAE}	0.0314	1.40	0.0293	1.19	0.0293	1.20	0.0291	1.20

simulations) were evaluated to assess the model performance of **model 2**, to confirm that the model established based on phase I data also fit for the phase II data. In addition, the normalized prediction distribution errors (NPDE) procedure[21,22] were applied. The NPDE values computed by NONMEM (using 1000 simulations) were plotted vs. time, time postdose, population predictions, and molecule indicator. The percentages of points below 10th percentile and above 50th and 90th percentiles were reported to assess the distribution of NPDE.

After qualification of **model 2**, the ability of the final integrated model to predict Tab concentration time course and PK exposure parameters (steady state area under the concentration-time curve [AUC], minimum concentration [C_{min}], and maximum concentration [C_{max}] following 2.4 mg/kg every 3-week bolus repeated dosing, computed using individual *post-hoc* PK parameters and the analytical solution for a two-compartment model) were evaluated. This evaluation was performed by comparing the predictions of individual Tab concentrations and exposure parameters estimated by **model 3** and **model 4** vs. **model 2** (the benchmarking scenario), using the goodness of fit plots and comparison of summary statistics.

RESULTS

Final integrated two-analyte population PK model

For **model 1** using phase I data, all model parameters (**Table 1**) were estimated with good precision (relative standard error [RSE]% $<$15%). Model diagnostic plots (**Supplemental Figure 1**) confirmed good agreement between the predicted and the observed phase I data with no systematic bias, suggesting that the final integrated model[18] with modifications is applicable to simultaneously describe the Tab and acMMAE clinical PK data. Differences in CL, V_C, k_{dec}, and CORR parameters for pinatuzumab vedotin and polatuzumab vedotin were 18%, 7%, 32%, and 10%, respectively, indicating that the PK of these two ADCs are largely similar, and the integrated model structure can apply to both molecules. The effect of time-dependent clearance is minimal (unpublished data, Genentech) and was not included in the final model.

When **model 1** was used to fit the combined data from phase I and II studies with parameters reestimated (**model 2**), the model diagnostic plots confirmed good agreement between the predicted and observed data with no systematic bias (**Supplemental Figure 2**). Parameter estimates of **model 1** and **model 2** were also similar (**Table 1**), indicating that the final model is applicable to describe both phase I and II data. Furthermore, the VPC plot for **model 2** indicated good agreement between the dose-normalized observed and simulated concentrations (**Supplemental Figure 3**). NPDE plots also indicated a distribution around line of zero with no systemic bias when plotted vs. time; time postdose, population predictions, and ADC type (**Figure 3**). The percentages of points below the 10th percentile and above the 50th and 90th percentiles were 6%, 52%, and 6%, respectively, suggesting a good agreement of the distribution between the observed and model-simulated data, so the model is able to reproduce both the central tendency and variability of observed data.

Model application for Tab PK sampling reduction or elimination

The final model was used to assess whether Tab concentrations can be predicted from observed acMMAE data, based on reduced or eliminated Tab PK concentrations. It was observed that the parameter estimates of **Models 2**, **3**, and **4** were similar (**Table 1**). Individual and population model predictions of Tab concentrations given no sampling of Tab PK (**model 3**) or sparse sampling of Tab PK (**model 4**) of phase II data were similar to the benchmark scenario of

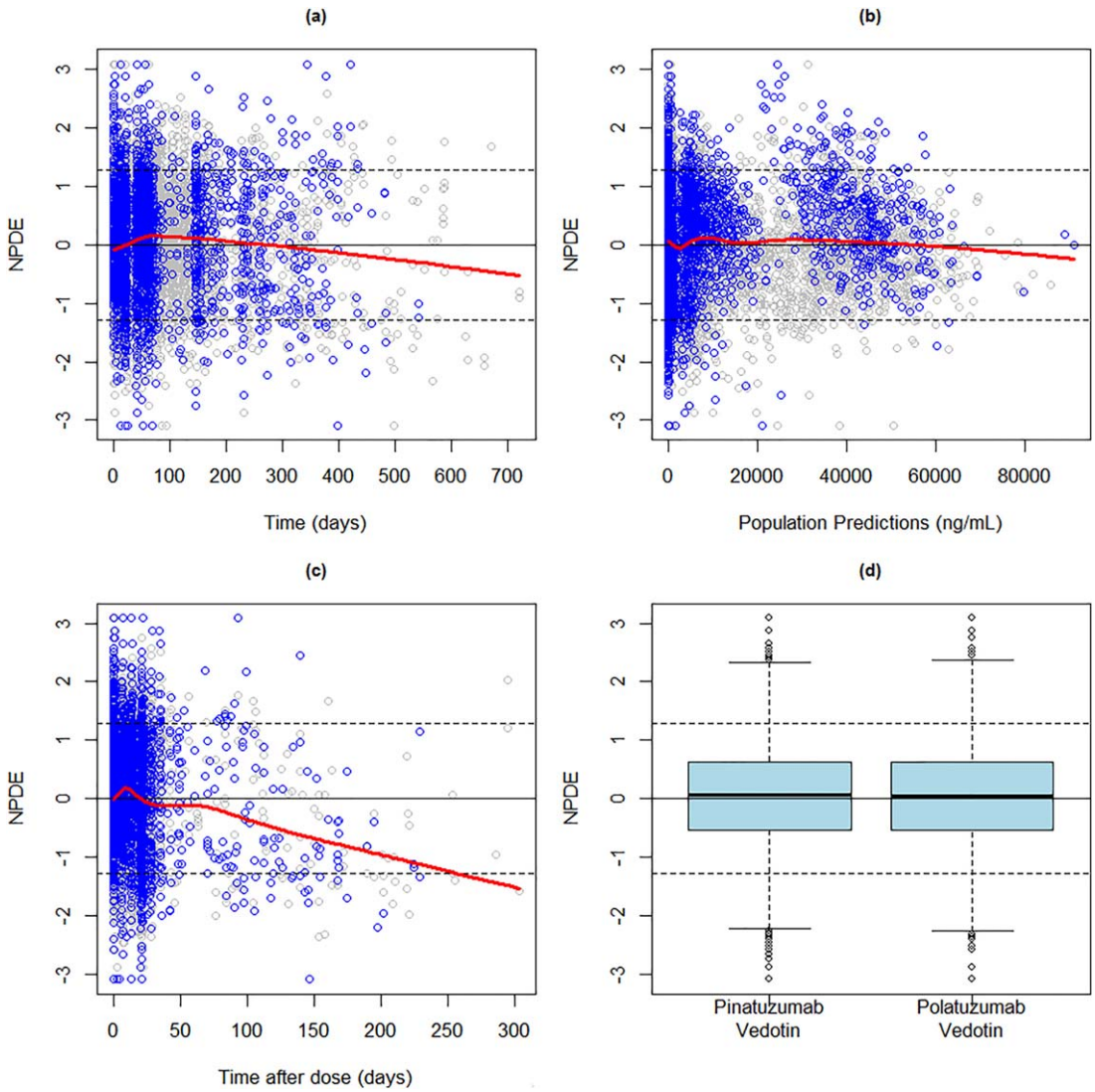

Figure 3 Evaluation of the final model for fitting combined phase I and II data (Model 2) by NPDE plot (both ADCs and both analytes combined) for NPDE vs. (**a**) time, (**b**) population predictions, (**c**) time after dose, and (**d**) pinatuzumab vedotin and polatuzumab vedotin. Phase I data: gray open circles; phase II data: blue open circles.

using all available data (**model 2**) (**Figure 4**). Furthermore, PK exposure estimates for Tab (steady-state AUC, C_{min}, and C_{max}) were similar, with the difference of mean values less than 17% for **model 3** compared to **model 2**, and less than 8% for **model 4** compared to **model 2,** across all three parameters (**Table 2** and **Figure 5**). These results suggested that removing the majority or all Tab PK samples in phase II did not appear to compromise the ability of the integrated Tab-acMMAE PK model to precisely estimate all PK exposure parameters of Tab, given the intensive sampling in phase I for both analytes and relatively dense sampling in phase II for acMMAE.

DISCUSSION AND CONCLUSIONS

The final integrated model allowed us to describe the correlations of two analytes (Tab and conjugate, measured by acMMAE) after ADC administration, using the combination of two linear two-compartment PK models for Tab and acMMAE that share the same parameters except that deconjugation constitutes an additional clearance pathway for acMMAE. Consequently, when the deconjugation rate is estimated based on phase I data of Tab and acMMAE, the observed PK of acMMAE in late-phase studies may be used to predict the PK of Tab. Reducing Tab PK sampling in late-phase clinical studies would reduce both patient burden and assay burden, which is also more cost-effective.

The models developed in this work contain a correction factor, CORR (Eq. 5) to correct a systemic bias in the model fitting. Theoretically, the mDAR of the dosing solution, which is used in the dose input for acMMAE and Tab, should be similar to or higher than the mDAR estimated by the molar ratio of observed PK concentrations of Tab and acMMAE at 30 minutes post end of infusion, at which timepoint the deconjugation is just starting to occur. However,

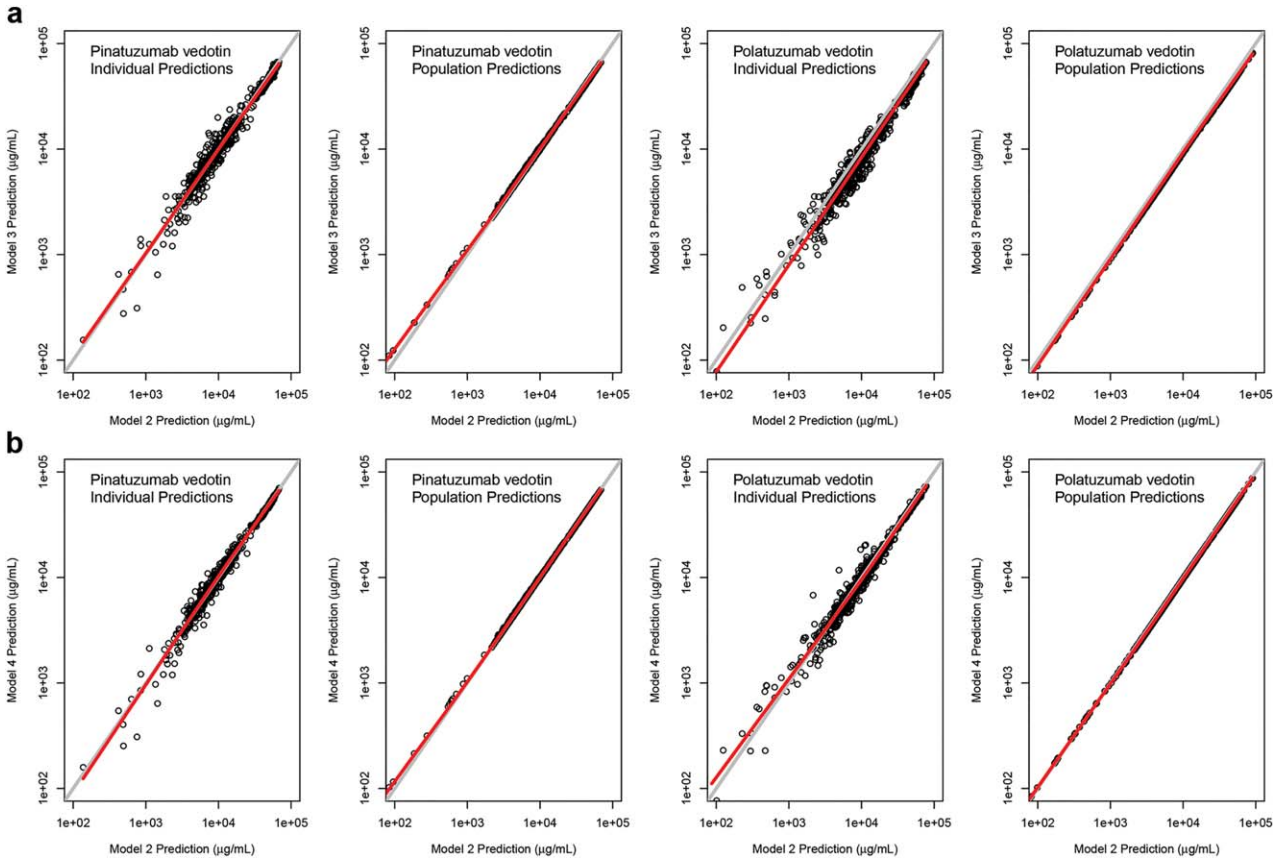

Figure 4 Comparison of model predictions of Tab concentrations (individual predictions and population predictions) for (**a**) Model 3 vs. Model 2 and (**b**) Model 4 vs. Model 2, for subjects from the phase II study for pinatuzumab vedotin and polatuzumab vedotin, respectively. Black open circles: each Tab PK data point for subjects from the phase II study; red line: LOESS smooth line.

the later values are systemically higher than the mDAR of the dosing solution, which caused the systemic bias in the model fitting. The most likely reason for this discrepancy may be related to the assay differences among these measurements. The mDAR of the ADC in the dosing solution was measured using an *in vitro* assay HIC. For clinical PK samples, Tab is quantified by a validated ELISA using an anti-CDR-specific antibody against anti-CD79b or anti-CD22 antibody as the capture reagent, and acMMAE is quantified by a validated LC-MS/MS method. The differential equations of the final PK model reported are initialized based on the mDAR determined by HIC, while the concentrations are quantified by the other two assays.

It is worth noting that the PK properties of two different ADCs with the same linker and cytotoxic drug can be described by the same structural model, with only minor differences in the model parameters. Possible reasons for this similarity include the fact that both ADCs have the same linker and drug components and are rapidly internalized upon binding. Prior analysis also suggested that the PK properties for the multiple MMAE-containing ADCs with the same linker are similar (Xu et al. http://www.acop7.org/previous-acop-meetings-acop6). Similar to the models for other mAbs that target B-cells,[23,24] both ADCs had a time-dependent clearance component that declined rapidly to zero within the first cycle (unpublished data, Genentech, and Lu et al., poster #PII-095, http://www.ascpt.org/Portals/8/docs/Meetings/2015%20Annual%20Meeting/Final%20Program%20-%20FINAL.pdf). However, the effect was minor and did not influence the conjugate PK beyond cycle 1. Given the purpose of this model, a simplified model is more desirable. Thus, the time-dependent change of clearance was not included.

The key model assumptions were that the proteolytic clearance of each DAR species is DAR-independent, and the deconjugation rate of each DAR species was linearly proportional to the DAR. The proteolytic clearance is mainly composed of target-mediated clearance and nonspecific clearance. Based on the binding affinity values measured *in vitro*, the antibody of the ADC maintains antigen binding integrity and affinity after conjugation (unpublished data, Genentech). Thus, the target-mediated clearance is expected to be similar for individual DAR species. However, conjugation appears to increase the nonspecific clearance, as indicated by a faster total clearance of Tab (https://ash.confex.com/ash/2013/webprogram/Paper62229.html)[13] (8–20 mL/day/kg) compared to the clearance of typical mAbs of ~3–6 mL/day/kg.[25] It is also not known whether the high DAR species have a higher nonspecific clearance compared to the low DAR species. Considering that only the total concentrations of Tab

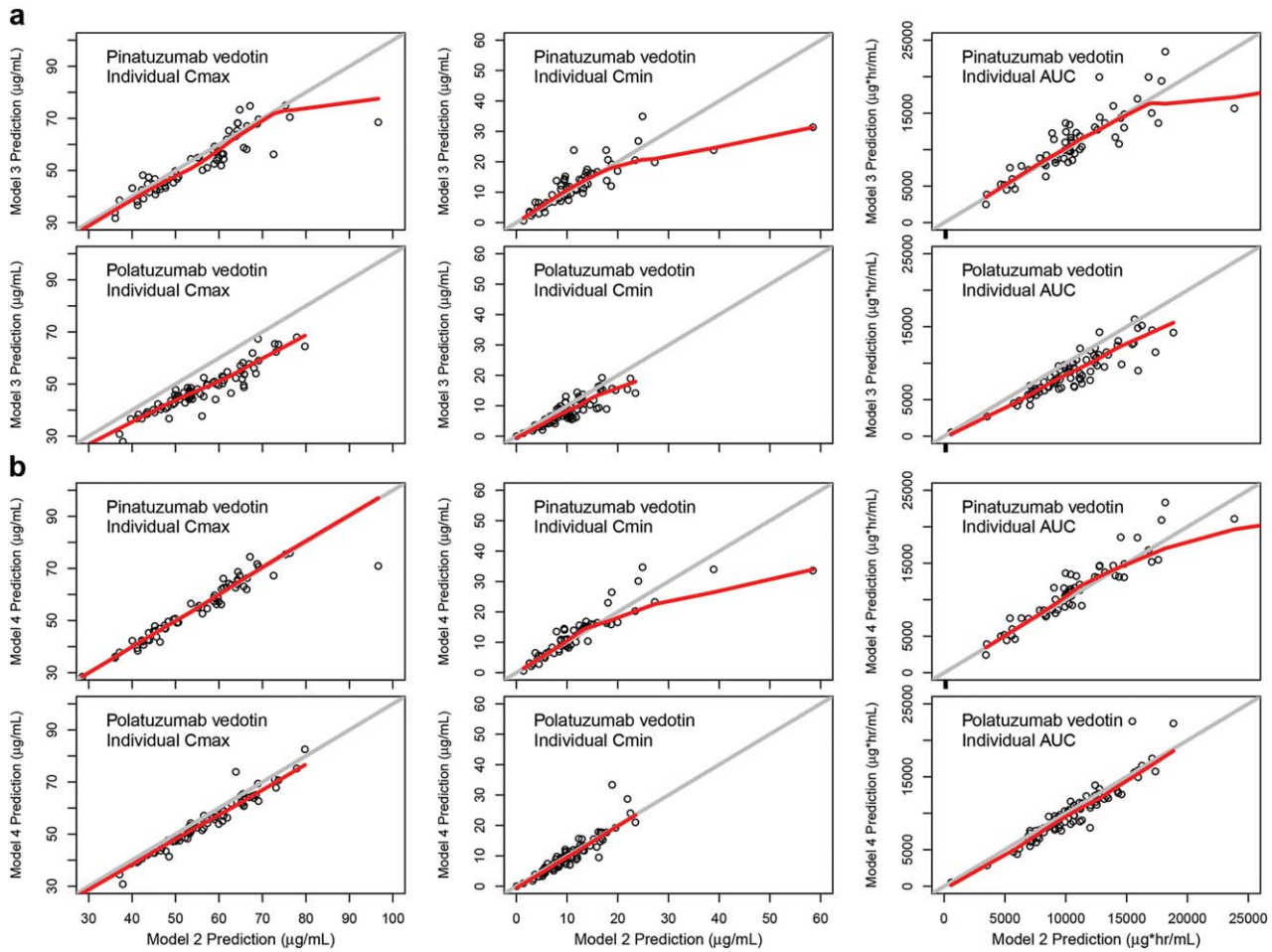

Figure 5 Comparison of model-predicted Tab PK exposure parameters (C_{max}, C_{min}, and AUC) at steady state for (**a**) Model 3 vs. Model 2 and (**b**) Model 4 vs. Model 2, for subjects from the phase II study for pinatuzumab vedotin and polatuzumab vedotin, respectively. Black open circle: PK exposure parameter of each individual patient from the phase II study; red line: LOESS smooth line.

and acMMAE (both are mixtures of different DAR species) are quantified in clinical studies without the data of individual DAR species, previous analysis[18] suggested the model for estimating DAR-dependent proteolytic clearance would have model parameter identifiability issues. Thus, a simplified model was used for the current analysis. A more mechanistic model to allow both DAR-dependent proteolytic clearance and deconjugation, such as the model used to fit the preclinical data for a thiomab-drug-conjugate,[17] could be applied when the concentrations of individual DAR species are quantified.

Given the major goals of this integrated modeling, a relatively simple population PK model without covariates was used. The model diagnosis indicated good individual

Table 2 Summary statistics of estimated Tab PK parameters (AUC, C_{min}, and C_{max}) for the phase II study based on all available Tab data (**model 2**), no Tab data (**model 3**), and sparse Tab data (**model 4**).

	Mean (SD)			Median (range)		
Model	**AUC (µg*hr/mL)**	**C_{min} (µg/mL)**	**C_{max} (µg/mL)**	**AUC (µg*hr/mL)**	**C_{min} (µg/mL)**	**C_{max} (µg/mL)**
All Tab data were used in individual estimates (Model 2)						
CD22	11034 (5012)	12 (9)	55 (12)	10308 (3439–34784)	10 (1.4-58)	56 (29-97)
CD79b	10524 (3264)	10 (5)	55 (10)	10402 (579–18841)	10 (0.1-23)	54 (25-80)
Phase II Tab data were not used (Model 3)						
CD22	11008 (4330)	12 (7)	53 (11)	10432 (2486–23463)	12 (0.6-35)	53 (26-75)
CD79b	8730 (2983)	9 (4)	48 (9)	8548 (529–16024)	8 (0-19)	47 (23-68)
Limited phase II Tab data were used (Model 4)						
CD22	11263 (4487)	13 (8)	55 (11)	11149 (2481–23327)	11 (0.6-35)	56 (29-76)
CD79b	10085 (3749)	10 (6)	53 (10)	9679 (558–22619)	9 (0.1-33)	53 (24-83)

predictions (IPRED) for all subjects regardless of the key covariates such as body weight. Thus, the model predictive performance of Tab PK, which is based on IPRED (**Table 2**), would not be affected by using a model without covariates. Covariate assessment was performed for the acMMAE population PK model (https://ash.confex.com/ash/2015/webprogram/Paper78428.html, Lu et al., poster #PII-095, http://www.ascpt.org/Portals/8/docs/Meetings/2015%20Annual%20Meeting/Final%20Program%20-%20FINAL.pdf). Following polatuzumab vedotin dosing, baseline B-cell count, tumor burden, body weight, and sex were statistically significant covariates for acMMAE clearance, while body weight and sex were statistically significant covariates for acMMAE central volume of distribution.

It is also important to understand the PK of unconjugated MMAE in relation to Tab and acMMAE, given that unconjugated MMAE is a key catabolite after ADC administration. Thus, population PK modeling to integrate the PK of unconjugated MMAE is being developed and will be reported separately.

In summary, an integrated population PK model was established to simultaneously fit the PK of Tab and acMMAE after dosing of MMAE-containing ADCs (pinatuzumab vedotin and polatuzumab vedotin) in patients with B-cell lymphoma. The established model based on intensive PK sampling from phase I studies successfully described the PK of Tab and the acMMAE of the two ADCs tested. The model also demonstrated its ability to predict Tab PK parameters and concentrations based on observed acMMAE PK with no Tab PK sampling or reduced Tab PK sampling. Thus, the model can be used to significantly reduce (more than 80%) or even completely eliminate Tab sampling in late-phase clinical studies without compromising PK characterization. This model is likely applicable for the entire MMAE ADC platform.

Acknowledgments. The authors thank all the principal investigators and patients for their participation and contribution to the phase I studies for pinatuzumab vedotin and polatuzumab vedotin, and the phase II study. The authors thank Anshin Biosolutions and Envision Pharma, Inc. for their editorial support of the article.

Conflict of Interest. The analysis was funded by Genentech, Inc., a member of the Roche group. All of the authors, except Leonid Gibiansky, are employees of Genentech, Inc. and stockholders of the Roche group. Leonid Gibiansky is a paid consultant for Roche and Genentech.

Author Contributions. D.L., S.G., A.J., J.Y.J. , C.L., J.H. and Y-W.C. designed the research, D.L., L.G., P.A., R.D., J.H. and Y-W.C. performed the research; D.L., L.G. and S.G. wrote the manuscript; all authors reviewed, edited and approved the manuscript.

1. Hughes, B. Antibody-drug conjugates for cancer: poised to deliver? *Nat. Rev. Drug Discov.* **9**, 665–667 (2010).
2. Prabhu, S. *et al.* Antibody delivery of drugs and radionuclides: factors influencing clinical pharmacology. *Ther. Deliv.* **2**, 769–791 (2011).
3. Mullard, A. Maturing antibody-drug conjugate pipeline hits 30. *Nat. Rev. Drug Discov.* **12**, 329–332 (2013).
4. Bouchard, H., Viskov, C. & Garcia-Echeverria, C. Antibody-drug conjugates-a new wave of cancer drugs. *Bioorg. Med. Chem. Lett.* **24**, 5357–5363 (2014).
5. Teicher, B.A. & Chari, R.V. Antibody conjugate therapeutics: challenges and potential. *Clin. Cancer Res.* **17**, 6389–6397 (2011).
6. Kaur, S., Xu, K., Saad, O.M., Dere, R.C. & Carrasco-Triguero, M. Bioanalytical assay strategies for the development of antibody-drug conjugate biotherapeutics. *Bioanalysis* **5**, 201–226 (2013).
7. Lu, D. *et al.* Semi-mechanistic multiple-analyte pharmacokinetic model for an antibody-drug-conjugate in cynomolgus monkeys. *Pharm. Res.* **32**, 1907–1919 (2015).
8. Shen, B.Q. *et al.* Conjugation site modulates the in vivo stability and therapeutic activity of antibody-drug conjugates. *Nat. Biotechnol.* **30**, 184–189 (2012).
9. Bender, B. *et al.* A mechanistic pharmacokinetic model elucidating the disposition of trastuzumab emtansine (T-DM1), an antibody-drug conjugate (ADC) for treatment of metastatic breast cancer. *AAPS J.* **16**, 994–1008 (2014).
10. Gorovits, B. *et al.* Bioanalysis of antibody-drug conjugates: American Association of Pharmaceutical Scientists Antibody-Drug Conjugate Working Group position paper. *Bioanalysis* **5**, 997–1006 (2013).
11. Gorovits, B. & Shord, S. Novel methods in bioanalysis and characterization of antibody-drug conjugates. In *Novel Methods in Bioanalysis and Characterization of Antibody-Drug Conjugates* (eds. Gorovits, B. & Shord, S.) 2–4 (Future Medicine, London, UK, 2015).
12. Girish, S.R. & Li, C. Clinical pharmacology and assay consideration for characterizing pharmacokinetics and understanding efficacy and safety of antibody-drug conjugates. In *Novel Methods in Bioanalysis and Characterization of Antibody-Drug Conjugates* (eds. Gorovits, B. & Shord, S.) 36–55 (Future Medicine, London, UK, 2015).
13. Palanca-Wessels, M.C. *et al.* Safety and activity of the anti-CD79B antibody-drug conjugate polatuzumab vedotin in relapsed or refractory B-cell non-Hodgkin lymphoma and chronic lymphocytic leukaemia: a phase 1 study. *Lancet Oncol.* **16**, 704–715 (2015).
14. Shah, D.K. *et al.* A priori prediction of tumor payload concentrations: preclinical case study with an auristatin-based anti-5T4 antibody-drug conjugate. *AAPS J.* **16**, 452–463 (2014).
15. Chudasama, V.L. *et al.* Semi-mechanistic population pharmacokinetic model of multivalent trastuzumab emtansine in patients with metastatic breast cancer. *Clin. Pharmacol. Ther.* **92**, 520–527 (2012).
16. Lu, D. *et al.* An integrated multiple-analyte pharmacokinetic model to characterize trastuzumab emtansine (T-DM1) clearance pathways and to evaluate reduced pharmacokinetic sampling in patients with HER2-positive metastatic breast cancer. *Clin. Pharmacokinet.* **52**, 657–672 (2013).
17. Sukumaran, S. *et al.* Mechanism-based pharmacokinetic/pharmacodynamic model for THIOMAB drug conjugates. *Pharm. Res.* **32**, 1884–1893 (2015).
18. Gibiansky, L. & Gibiansky, E. Target-mediated drug disposition model and its approximations for antibody-drug conjugates. *J. Pharmacokinet. Pharmacodyn.* **41**, 35–47 (2014).
19. Lim, S.T. Antibody-drug conjugates in non-Hodgkin lymphoma. *Lancet Oncol.* **16**, 607–608 (2015).
20. Yano, Y., Beal, S.L. & Sheiner, L.B. Evaluating pharmacokinetic/pharmacodynamic models using the posterior predictive check. *J. Pharmacokinet. Pharmacodyn.* **28**, 171–192 (2001).
21. Brendel, K., Comets, E., Laffont, C., Laveille, C. & Mentre, F. Metrics for external model evaluation with an application to the population pharmacokinetics of gliclazide. *Pharm. Res.* **23**, 2036–2049 (2006).
22. Mentre, F. & Escolano, S. Prediction discrepancies for the evaluation of nonlinear mixed-effects models. *J. Pharmacokinet. Pharmacodyn.* **33**, 345–367 (2006).
23. Gibiansky, E. *et al.* Population pharmacokinetics of Obinutuzumab (GA101) in chronic lymphocytic leukemia (CLL) and non-Hodgkin's lymphoma and exposure-Response in CLL. *CPT Pharmacometrics Syst, Pharmacol.* **3**: e144 (2014).
24. Li, J. *et al.* Population pharmacokinetics of rituximab in patients with chronic lymphocytic leukemia. *J. Clin. Pharmacol.* **52**, 1918–1926 (2012).
25. Deng, R. *et al.* Projecting human pharmacokinetics of therapeutic antibodies from nonclinical data: what have we learned? *MAbs* **3**, 61–66 (2011).

Supplementary information accompanies this paper on the *CPT: Pharmacometrics & Systems Pharmacology* website (http://www.wileyonlinelibrary.com/psp4)